Engineering Structures 83 (2015) 154–162

Contents lists available at ScienceDirect

Engineering Structures

journal homepage: www.elsevier.com/locate/engstruct

Non-proprietary bar splice sleeve for precast concrete construction

Eliya Henin [a], George Morcous [b,*]

[a] Assiut University, Assiut, Egypt
[b] University of Nebraska–Lincoln, Omaha, NE, United States

ARTICLE INFO

Article history:
Received 18 April 2014
Revised 24 October 2014
Accepted 27 October 2014

Keywords:
Development length
Bond strength
Bar splice
Precast concrete
Confinement

ABSTRACT

Over the last few decades, the use of precast concrete components have been significantly increasing in building and bridge construction due to their quality, durability, and speed of construction. Precast components need to be fully connected to ensure the integrity, serviceability, and durability of the completed structure. Several proprietary grout-filled sleeves are currently being used to splice reinforcing bars of the adjacent precast components. These sleeves require very tight tolerances in precast production to ensure the alignment of the spliced bars, which usually results in using larger and more costly sleeves than needed. The objective of this paper is to introduce a non-proprietary bar splice sleeve that accommodates current production tolerances in addition to being economical and easy to produce. The design method of the proposed splice sleeve and the analytical investigation conducted using FE analysis are discussed. The experimental investigation conducted using two alternatives of the proposed bar splice sleeve is presented. Eighteen specimens for splicing #8 and #9 bars were tested using different sleeve lengths. Test results indicated that the proposed bar splice sleeve have adequate capacity to fully develop reinforcing bars while being simpler to use and more economical than current proprietary splice sleeves.

1. Introduction

Precast concrete construction usually requires connecting precast concrete components, such as wall panels, columns, and pier caps, to form the completed structure whether it is a building or bridge. Several proprietary grout-filled sleeves are currently being used to splice the reinforcing bars of adjacent components. Examples are NMB Splice Sleeve, Sleeve Lock by Dayton Superior, and Lenton Interlok. In these connections, sleeves are inserted around the reinforcing bar in one component during fabrication, while reinforcing bars are extended from the other component at the same location of the sleeves as shown in Fig. 1. During construction, the components are erected by inserting the projected bars from one component into the sleeves in the other component. Then, the sleeves are, then, filled with high strength non-shrink grout using grout vents and grout pump as shown in Fig. 1. Proprietary sleeves are designed to allow a maximum tolerance of ½” or less in the alignment of the spliced bars, which is a challenge to many precast producers. In these cases, they use the sleeves designed for one or two bar diameters larger than the diameter of the spliced bars to provide additional tolerance, which results in less efficient and more costly splicing.

The main objective of this paper are to introduce a non-proprietary bar splice sleeve that accommodates current production practices with respect to tolerances in addition to being easy to produce and more economical than existing proprietary sleeves. This includes developing an expression for calculating the required sleeve length as function of the bar diameter, grout strength, and desired tolerance. The paper is organized as follows: (a) previous research on the effect of transverse confinement on the bond strength of reinforcing bars is presented; (b) the concept and design of the proposed splice sleeve is discussed; (c) experimental investigation conducted to evaluate the proposed design is demonstrated as well as the analysis of test results; (d) theoretical investigation conducted sing finite element (FE) modeling is presented; and finally (e) research conclusions and recommendations are summarized.

2. Previous research

The structural performance and durability of reinforced concrete members are highly dependent on the bond strength between reinforcing steel bars and the surrounding concrete. Bond strength is a function of the confinement provided by the concrete itself and transverse reinforcement that surrounds reinforcing steel bars. Transverse confinement plays an important role in determining the required development length and/or splice length.

* Corresponding author.
E-mail address: gmorcous2@unl.edu (G. Morcous).

http://dx.doi.org/10.1016/j.engstruct.2014.10.045
0141-0296/

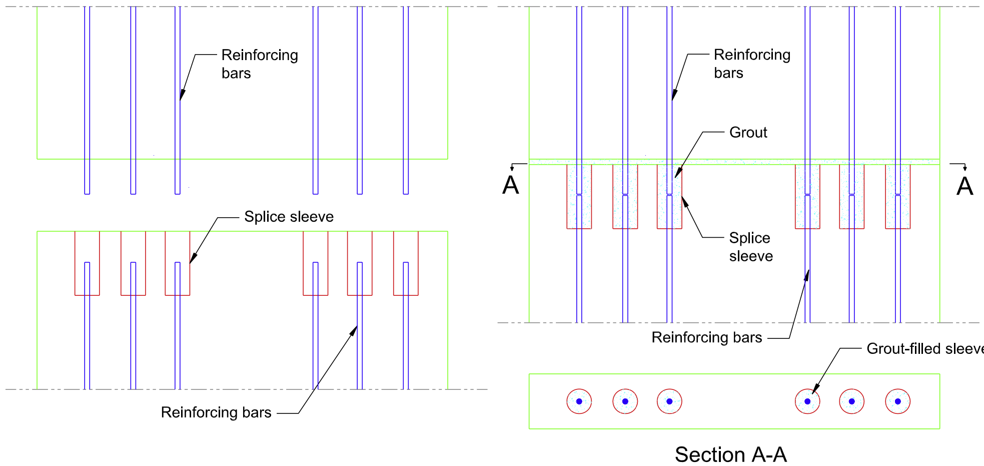

Fig. 1. Two precast concrete components before (left) and after (right) connecting using bar splice sleeves.

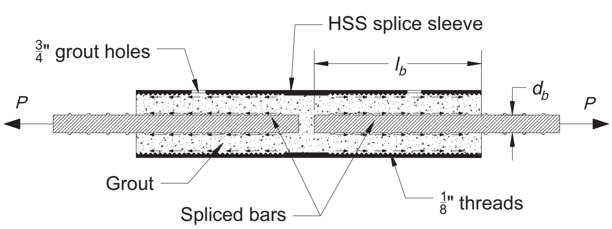

Fig. 2. Proposed bar splice sleeve and force transfer mechanism.

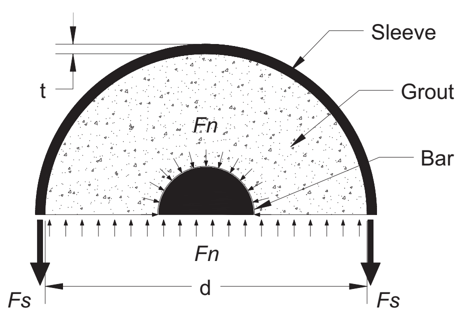

Fig. 3. Equilibrium of forces in the proposed bar splice sleeve.

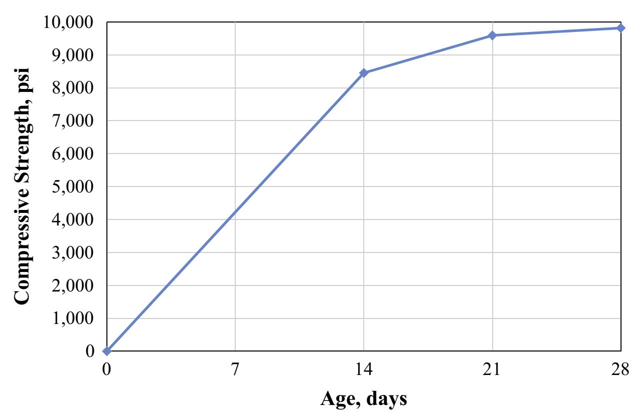

Fig. 4. Grout compressive strength development with time.

Transverse confinement have been studied extensively in several experimental and analytical investigations.

Untrauer and Henry [10] reported that the bond strength between the steel and concrete increases in proportion to square root of normal pressure and concrete strength. Normal pressure was applied to the faces of concrete specimens subjected to pullout forces. Orangun et al. [7] developed an expression for calculating the development and splice lengths for deformed bars with or without transverse reinforcement. These expressions were based on a nonlinear regression analysis of test results for beam specimens with lap splices that reflect the effect of splice length, concrete cover, bar diameter, concrete strength, and transverse reinforcement. The developed expression for the effect of transverse reinforcement was the basis for the current development length requirements in the ACI 318 [2]. Soroushian et al. [9] studied the effects of confinement by transverse reinforcement and compressive strength of concrete on local bond stress-slip characteristics of deformed bars using pullout testing. They reported that the ultimate bond strength increases almost proportionally with the square root of the concrete compressive strength. Confinement of concrete by transverse reinforcement did not directly influence the local bond behavior of deformed bars. Adajar et al. [1] established a new, simple and economical technique of connecting vertical bars in precast concrete shear walls by performing an experimental investigation using a combination of lapping bars and confining spirals. The effect of bar size, length of lapped bars, spacing of vertical bars, lug height of steel sheath, and pitch of spiral steel were studied. The main bars were spliced in grout-filled ducts that were surrounded by steel lapping bars and spiral. They concluded that the ultimate strength of the splices used in their investigation is equal to the tensile strength of the spliced bar when the lapping distance equals or exceeds 25 times the bar diameter. Sheikh and Toklucu [8] reported that the spiral reinforcement reached its yield strain before the confined concrete reached its maximum compressive strength, and the ultimate strength of the member increased with increased spiral yield strength. Also, they recommended using high strength wires to enhance reinforcement confinement of concrete. Einea et al. [4] evaluated the bond strength of reinforcing bars as a function of grout compressive strength and the level of confinement by studying the variables that affect the bond strength of reinforcing bars confined with steel pipes. They reported that a development length as short as seven time the bar diameter can be achieved by confining the high strength grout surrounding the bars. Darwin et al. [3] concluded that the fourth root of the concrete strength provided an accurate representation of the effect of concrete strength on bond

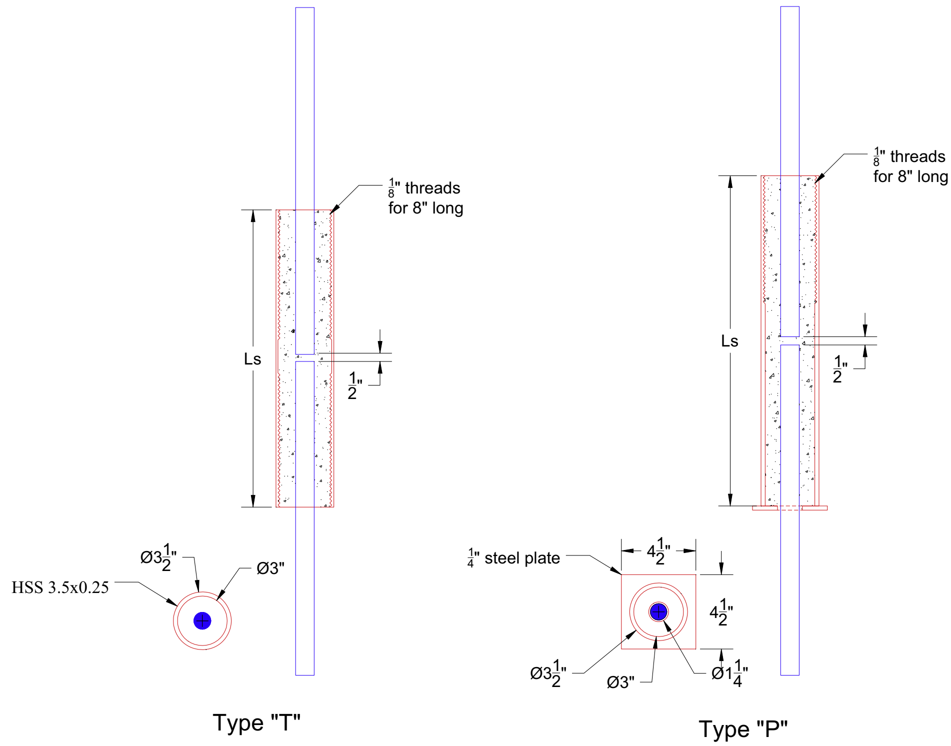

Fig. 5. Two types of the tested bar splice sleeves.

Table 1
List of specimens and their description.

Specimen ID	Bar size	Sleeve length (Ls), in.	Sleeve type	Number of specimens
8T16	# 8	16	T	2
8P16	# 8	16	P	2
8T18	# 8	18	T	2
8P18	# 8	18	P	2
8T20	# 8	20	T	2
9T16	# 9	16	T	2
9P16	# 9	16	P	2
9T20	# 9	20	T	2
9P20	# 9	20	P	2
			Total	18

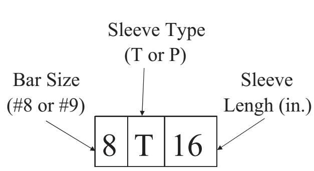

Fig. 6. Specimen identification system.

strength, and the yield strength of transverse reinforcement plays no significant role in determining the development length. Einea et al. [5] investigated the behavior of spirally confined lap splices of deformed reinforcing bars in concrete. They concluded that splices with two lapping bars attached to the main bars showed the best performance. Also, they reported that the ACI equation overestimates the required lap length by at least 76%. They recommended to waive the 12 in. limit on minimum length of a lap splice and increase the limit on the confinement term to 4 instead of 2.5. Zuo and Darwin [11] concluded that fourth root of the concrete strength and three-fourth root of the concrete strength are the best description of the effect of the concrete strength on splice length in cases of confinement with transverse reinforcement and non-confined concrete respectively. Also, they reported that the ACI limits on the confinement term are to ensure splitting failure, rather than pullout failure.

3. Proposed splice sleeve and design methodology

The proposed bar splice sleeve is simply a grout-filled round HSS (i.e. pipe) that has specific length, diameter, and thickness depending on the size of the bars being spliced. The sleeve is designed using the shear friction theory to transfer the force from one bar to the grout, then from the grout to the steel pipe, then from the steel pipe to the grout again, and finally from the grout to the other bar as shown in Fig. 2. The bond between the bar and grout is developed primarily by friction due to deformations on the bar surface and enhanced by the conferment effects of the pipe. The bond between the inside surface of the pipe and grout is developed primarily by friction through the threading of HSS inside surface using 1/8 in. threads as shown in Fig. 2. Two 3/4 in. diameter grout holes are provided: one to pump high strength non-shrink grout, and the other for air venting and quality assurance while grouting.

To determine the required embedment length (l_b) of a bar with given diameter (d_b) and force (P), the following equation is obtained based on equilibrium of forces:

$$l_b = \frac{P}{\pi d_b F_b} \quad (1)$$

where F_b is the bond strength between the bar and the surrounding grout.

Based on the shear friction theory, this bond strength can be estimated as the radial confinement stress (F_n), which is normal to the bar direction multiplied by the coefficient of friction (μ) between the bar and the grout, which can be assumed 1.0 for design purpose due to roughened (i.e. deformed) bar surface.

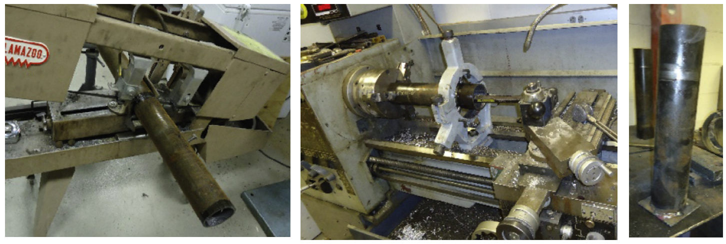

(a) Cut and thread the sleeve, then weld the end plate

(b) Install the bars, grout the sleeve, and make grout cubes

(c) Install the strain gauges

Fig. 7. Steps of specimen fabrication.

$$F_b = F_n \mu \tag{2}$$

To estimate the radial confinement stress (F_n), the equilibrium of forces in one unit-long section of the half sleeve shown in Fig. 3, results in:

$$F_n d = 2tF_s$$

$$F_n = \frac{2tF_s}{d} \leqslant 0.2f'_c \tag{3}$$

where F_s, t, and d are the yield stress, wall thickness, and inside diameter of the sleeve respectively. It should be noted that the radial confinement stress should not exceed $0.2f'_c$, (f'_c is compressive strength of grout) to limit the bearing stresses and avoid crushing failure of grout [6].

Therefore, the required embedment length of spliced bars using the proposed splice sleeve can be predicted using Eqs. (1)–(3) and simplified as shown below:

$$l_b = \frac{P}{\pi d_b \mu \min\left(0.2f'_c, \frac{2tF_s}{d}\right)} \tag{4}$$

The required sleeve length (l_s) will be at least twice the embedment length (l_b) rounded up to the nearest inch. For example, the embedment length of a Grade 60 ksi #9 bar in a round HSS 3.5 × 0.25 sleeve that has a yield strength of 42 ksi and filled with 10 ksi grout is calculated as follows:

$$P = 60 \times 1.0 = 60 \text{ kip}$$
$$d = 3.5 - 2 \times 0.25 = 3.0 \text{ in.}$$
$$\min\left(0.2f'_c, \tfrac{2tF_s}{d}\right) = \min\left(2, \tfrac{2\times0.25\times42}{3}\right) = 2 \text{ ksi}$$
$$l_b = \tfrac{60.0}{\pi\times1.128\times1.0\times2} = 8.47 \text{ in.} \approx 8.5 \text{ in.}$$
$$l_s = 2 \times 8.5 = 17 \text{ in.}$$

4. Experimental investigation

To evaluate the performance of the proposed bar splice sleeve, 18 pullout specimens were made using A615 Grade 60 #8 and #9 bars with different splice lengths. Bars have a minimum yield strength of 60 ksi and minimum ultimate strength of 90 ksi. All

Fig. 8. Pullout test setup.

specimens were made using A500 Grade B round HSS 3.5 × 0.25 sleeve that has a minimum yield strength of 42 ksi, minimum ultimate strength of 58 ksi, and nominal wall thickness of 0.25 in. (actual wall thickness is 0.233 in). All specimens were grouted using a cement-based metallic-aggregate mortar that has non-shrink, high strength, and high fluidity properties. Fig. 4 shows the development of grout compressive strength with time using the average of testing three 2 in. cubes. The average compressive strength at 28 days was 9812 psi.

Two types (alternatives) of bar splice sleeves were investigated as shown in Fig. 5: type "T" which represents sleeves that are internally threaded from both ends; and type "P" represents sleeves that are internally threaded from one end only, while the other end has a welded square steel plate with a centered hole for the splice bar. Type "T" sleeve is symmetrical and, therefore, can be used in either side. Type "P" sleeve has to be used so that the threaded end is located at the face of the precast connection where tolerances are needed. The end of the welded plate is embedded in the precast component where the bar is pre-installed and no tolerances are needed. This type was developed as a lower cost option as the cost of welded plate is slightly lower than that of threaded sleeve. Table 1 lists the description of the 18 specimens in terms of bar size, sleeve length, and sleeve type. Fig. 6 also shows the labeling system used for specimen identification. It should be noted that the use of a smooth sleeve without threading or welded plate was investigated at the early stage of this study. However, this option was eliminated due to the premature slippage of the grout from the sleeve at very low loads.

Specimens were fabricated, as shown in Fig. 7, in three main steps:

a. Cut the HSS section to the required sleeve length and thread the inside surface of the sleeve from one end for type "P" specimens and from both ends for type "T" specimens. Then, weld the end plate for type "P" specimens.
b. Install the bars to be spliced, then, pour the mortar to grout the sleeves. At least six grout cubes are made to evaluate the grout compressive strength.
c. After the grout reaches the required compressive strength, two electrical resistance strain gauges are placed on each end of the sleeve: one gauge is placed in the tangential direction to measure the hoop strains, and the other gauge is placed in the longitudinal direction to measure the tensile strains in the sleeve while pullout testing.

Specimens were tested as shown in Fig. 8 using Tinius Olsen universal testing machine. Bars were gripped using wedges and pulled out gradually at a constant rate of 0.001 in/min. Strains and displacements were recorded as the load increased using 16-channel MEGADAC data acquisition system. Maximum pullout forces, corresponding stresses, and failure modes are listed in Table 2 for the 18 specimens. The table also presents the calculated

Table 2
Summary of test results.

Specimen ID	Failure mode	Maximum load (P), kip	Maximum stress (ksi)	Ratio of maximum-to-yield stress[a]	Ratio of maximum-to-ultimate stress[a]
8T16	Pullout	87.1	110.25	1.84	1.23
8T16	Rupture	87.4	110.63	1.84	1.23
8P16	Pullout	87.3	110.51	1.84	1.23
8P16	Pullout	87.3	110.51	1.84	1.23
8T18	Rupture	87.6	110.89	1.85	1.23
8T18	Rupture	87.2	110.38	1.84	1.23
8P18	Rupture	87.7	111.01	1.85	1.23
8P18	Rupture	87.5	110.76	1.85	1.23
8T20	Rupture	87.6	110.89	1.85	1.23
8T20	Rupture	85.0	107.59	1.79	1.20
9T16	Pullout	92.0	92.00	1.53	1.02
9T16	Pullout	89.2	89.20	1.49	0.99
9P16	Pullout	102.6	102.60	1.71	1.14
9P16	Pullout	101.4	101.40	1.69	1.13
9T20	Rupture	104.3	104.30	1.74	1.16
9T20	Rupture	104.2	104.20	1.74	1.16
9P20	Rupture	97.9	97.90	1.63	1.09
9P20	Rupture	97.9	97.90	1.63	1.09
Minimum			89.2	1.49	0.99
Maximum			111.0	1.85	1.23
Average			105.2	1.75	1.17
Coefficient of variation			6.7%	6.7%	6.7%

[a] Yield stress is assumed 60 ksi and ultimate stress is assumed 90 ksi.

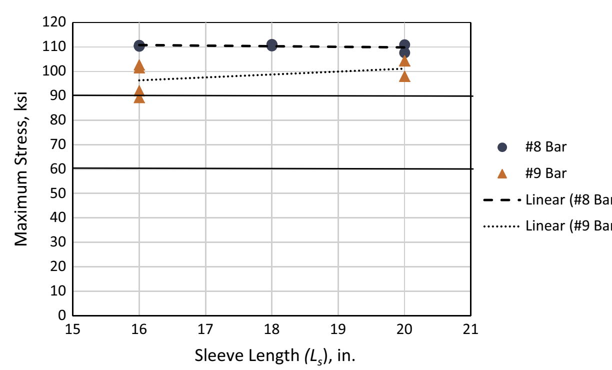

Fig. 10. Maximum bar stress versus sleeve length for different bar sizes.

Fig. 9. Failure modes. Bar rupture (left) and bar pullout (right).

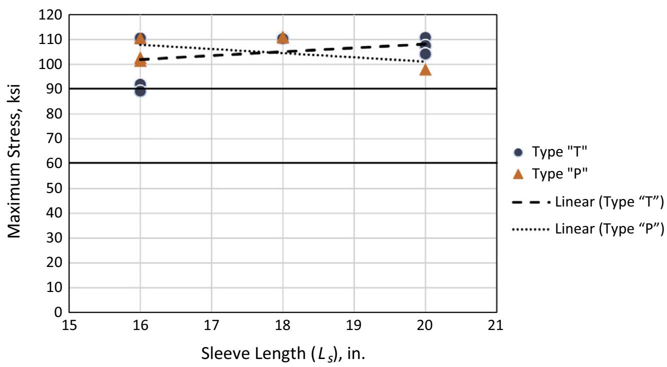

Fig. 11. Maximum bar stress versus sleeve length for different sleeve type.

ratios of maximum stresses to yield and ultimate stresses. These ratios indicate that the proposed bar splice sleeve did not only achieve the yield stress of the bars, but also the ultimate stress of the bars in all specimens. Two modes of failure were observed in this investigation: pullout and rupture of the bars as shown in Fig. 9. Specimens with pullout failure mode are highlighted in Table 2, which indicates that this mode of failure was limited to specimens with short sleeve length (16 in.) Figs. 10 and 11 plot the test results for different bar sizes and sleeve types respectively. Fig. 10 indicates that maximum stresses in #8 bar are almost constant and independent of the sleeve length, while maximum stresses in #9 bars are scattered and increases as the sleeve length increases. Fig. 11 indicates that type "P" sleeve is more effective than type "T" sleeve for short sleeve length and vice versa for longer sleeve length.

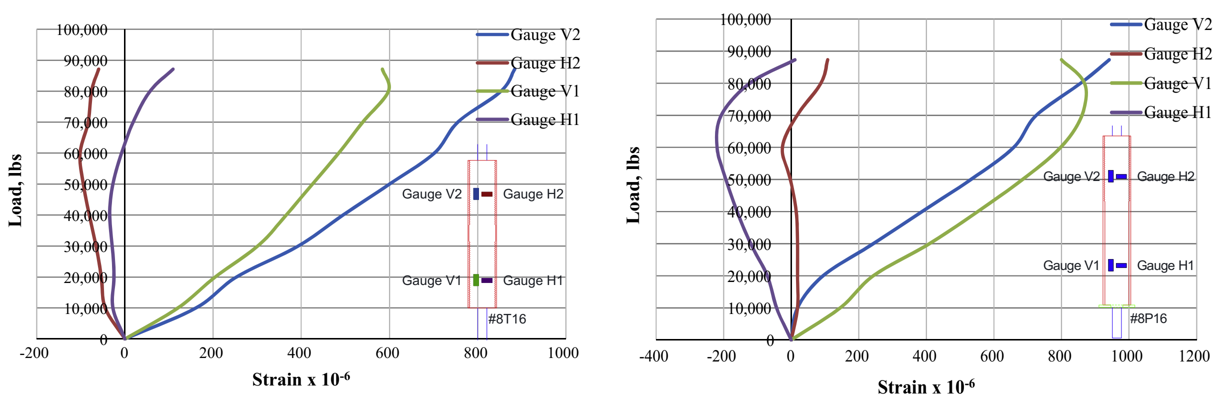

Fig. 12. Load–strain relationship for 8T16 and 8P16 specimens.

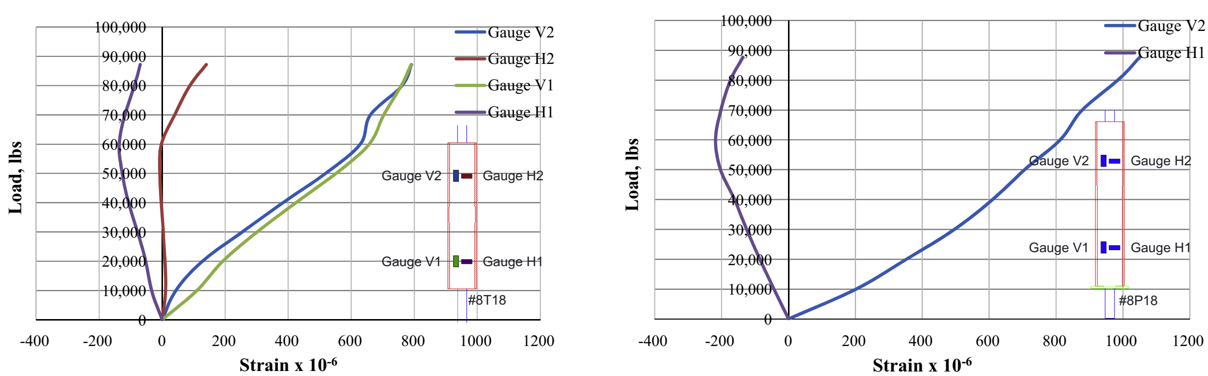

Fig. 13. Load–strain relationship for 8T18 and 8P18 specimens.

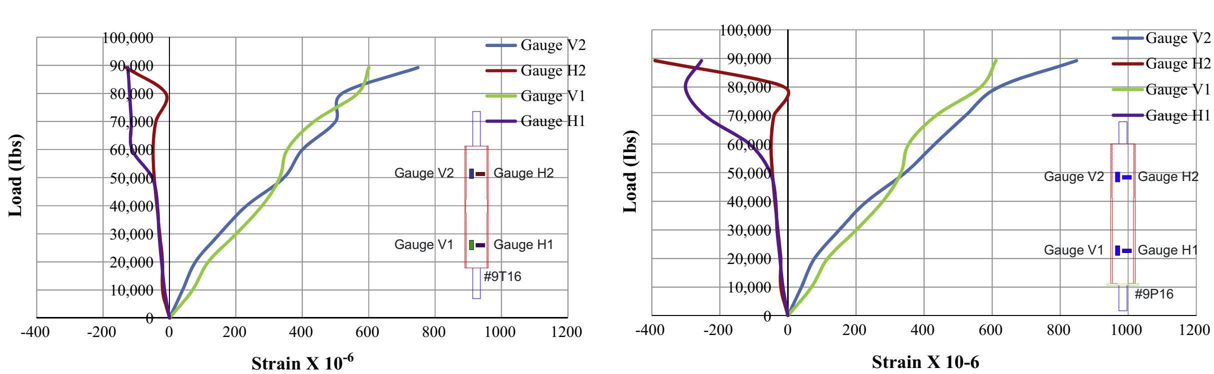

Fig. 14. Load–strain relationship for 9T16 and 9P16 specimens.

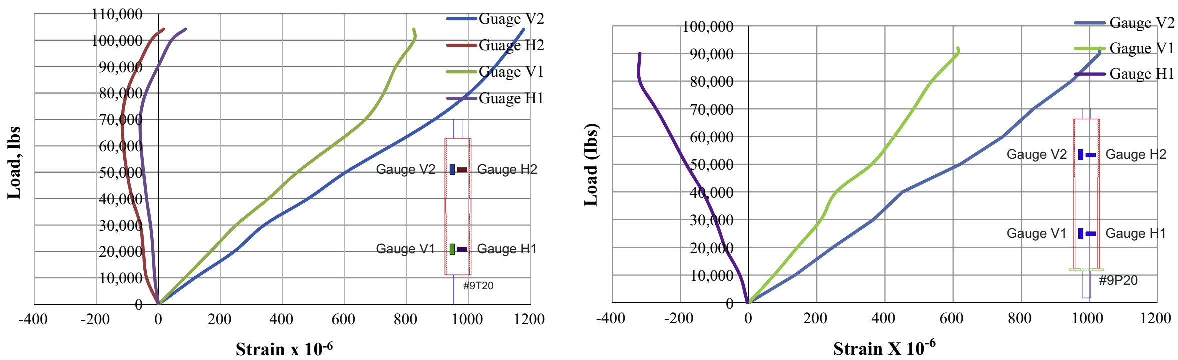

Fig. 15. Load–strain relationship for 9T20 and 9P20 specimens.

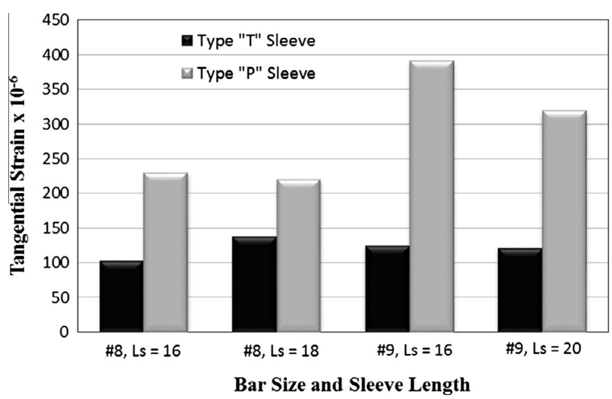

Fig. 16. Tangential strain measurements for types "T" and "P" sleeves.

Longitudinal and tangential strains in the pipe are plotted in Figs. 12–15 as a function of the applied loads. These figures indicate that the tangential strain are negative (i.e. compression) due to the passion effect as the sleeve is subjected to tension in the longitudinal direction. The maximum tangential strain is -390×10^{-6}, which is significantly less than the yield strain 1448×10^{-6} and corresponds to a tangential compressive stress of 11.3 ksi. Also, the figures indicate that as the bars start yielding, the tangential compressive strains in the sleeve decrease and change to tensile strains, which reflects the confinement effects in the sleeve. Longitudinal strains increase with the applied load up to failure. The maximum longitudinal strain in the pipe reached approximately 1190×10^{-6}, which is also less than the yield strain and corresponds to a tensile stress of 34.5 ksi. All strain measurements indicated that the sleeves did not reach the yield stress in either tangential or longitudinal directions.

By plotting the maximum tangential strains in the tested sleeves for types "T" and "P" as shown in Fig. 16, it can be clearly observed that strains in type "P" sleeves are higher than those of type "T" sleeves. This can be attributed to the restraining effects of the welded plates at one end of the sleeve, which results in a non-uniform distribution of strains along the sleeve. Table 3 presents calculated values of average bond strength and coefficient of friction based on the maximum tensile forces obtained from testing 18 specimens. In designing the sleeve, coefficient of friction coefficient was assumed to be 1.0 and the confinement stress was limited to 0.2 fc' in order to achieve the yield strength of the spliced bars. However, all spliced bars have achieved or exceeded the ultimate strength, which means that either coefficient of friction, confinement stress, or both are higher than predicted. Table 3 lists the coefficient of friction for each specimen assuming that the confinement stress is limited to $0.2 \times 9.8 = 1.95$ ksi. This assumption is validated by the analytical investigation presented in the next section.

Table 3
Calculated bond strength and coefficient of friction based on test results.

Specimen ID	Bar diameter (d_b) (in.)	Sleeve length (L_s) (in.)	Maximum load (P), kip	Average bond strength (F_b) (ksi)	Coefficient of friction (μ)
8T16	1	16	87.1	3.47	1.77
8T16	1	16	87.4	3.48	1.77
8P16	1	16	87.3	3.47	1.77
8P16	1	16	87.3	3.47	1.77
8T18	1	18	87.6	3.10	1.58
8T18	1	18	87.2	3.08	1.57
8P18	1	18	87.7	3.10	1.58
8P18	1	18	87.5	3.09	1.58
8T20	1	20	87.6	2.79	1.42
8T20	1	20	85.0	2.71	1.38
9T16	1.128	16	92.0	3.25	1.66
9T16	1.128	16	89.2	3.15	1.61
9P16	1.128	16	102.6	3.62	1.85
9P16	1.128	16	101.4	3.58	1.82
9T20	1.128	20	104.3	2.94	1.50
9T20	1.128	20	104.2	2.94	1.50
9P20	1.128	20	97.9	2.76	1.41
9P20	1.128	20	97.9	2.76	1.41
Minimum				2.7	1.38
Maximum				3.6	1.85
Average				3.2	1.61
Coefficient of variation				9.6%	9.6%

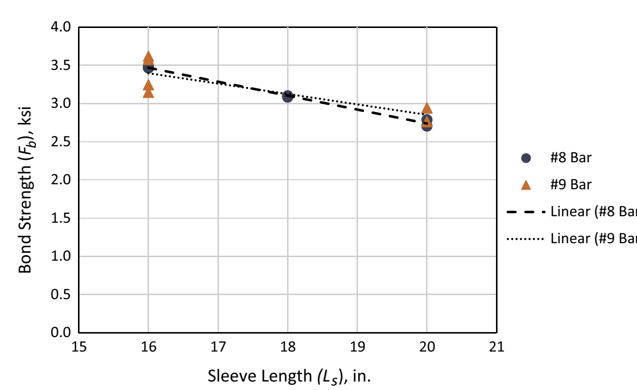

Fig. 17. Relationship of bond strength and sleeve length for different bar sizes.

Fig. 17 plots the relationship between the average bond strength (F_b) calculated in Table 3 and the sleeve length (L_s) for different bar sizes. This plot indicates that the relationship is linear and has a constant slope of 0.16 ksi per in. regardless of the bar size.

5. Analytical investigation

Two 3D finite element (FE) models were developed to analytically investigate the structural behavior of the proposed splice sleeve of types “T” and “P”. The two models were developed for specimens 8T18 and 8P18 using ANSYS program as shown in Fig. 18. In these models, grout was modeled using SOLID65 elements capable of simulating the cracking and crushing of brittle materials, while steel sleeve and bars were modeled using SOLID185 elements suitable for ductile materials. Stress–strain relationships of grout, sleeve, and bars were used to define the mechanical properties of each material. The interfaces between grout and sleeve, and grout and bars were modeled using contact elements. Different values for the coefficient of friction were assumed to evaluate the sensitivity of the model output to this parameter and determine the value that results in a failure load and mode that are consistent with the experimental investigation. The double symmetry of the two models was utilized in the analysis to reduce the computation time significantly.

Fig. 19 shows the stress distribution on the quarter specimens at failure. The distribution indicates that stresses are the highest around the bars and they decrease gradually to the lowest at the tube. It also indicates that stresses in the type “T” sleeves are slightly higher than those in Type “P” sleeves. The FE analysis has indicated that coefficients of friction of 1.6 and 1.7 result in the actual failure load and mode observed for specimens 8T18 and 8P18 respectively. These values are very close to those presented in Table 3. Stress results also indicates the adequacy of the 0.2 f_c' limit on the confinement stress to avoid excessive deformation of the surrounding grout.

6. Conclusions

The non-proprietary bar splice sleeve system proposed for precast concrete construction is economical, easy to produce, and

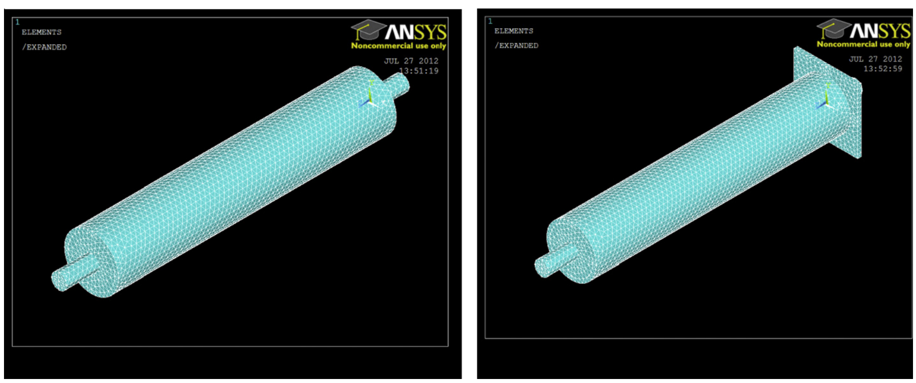

Fig. 18. FE models for 8T18 (left) and 8P18 (right) specimens.

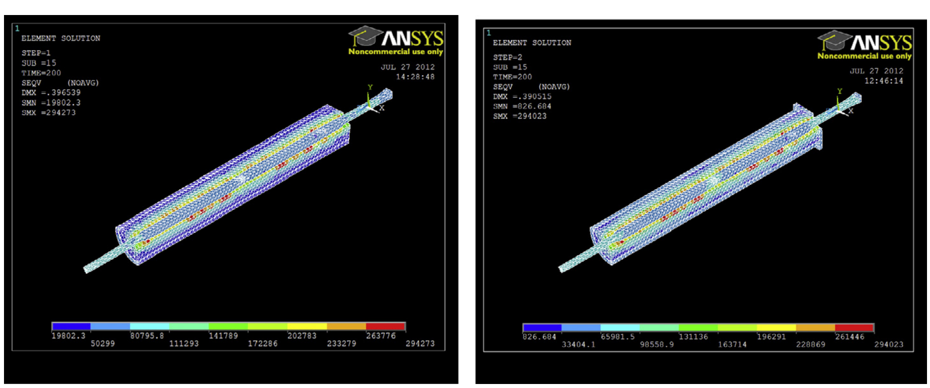

Fig. 19. Stress distribution in 8T18 (left) and 8P18 (right) specimens.

Table 4
Recommended sizes of splice sleeves for different bar sizes.

Spliced bars			Recommended splice sleeve					
Size	Diameter (in.)	Area (in.^{2})	Size	Weight (lb/ft)	Area (in.^{2})	Inside Diameter (in.)	Tolerance (in.)	Length (in.)
#6	0.750	0.440	HSS 3.0 × 0.188	5.7	1.54	2.65	0.95	12
#7	0.875	0.600	HSS 3.0 × 0.188	5.7	1.54	2.65	0.89	14
#8	1.000	0.790	HSS 3.5 × 0.25	8.7	2.39	3.03	1.02	16
#9	1.128	1.000	HSS 3.5 × 0.25	8.7	2.39	3.03	0.95	18
#10	1.270	1.270	HSS 4.0 × 0.25	10.0	2.76	3.53	1.13	20
#11	1.410	1.560	HSS 4.0 × 0.313	12.3	3.39	3.42	1.01	23
#14	1.693	2.250	HSS 4.5 × 0.337	15.0	4.12	3.87	1.09	27
#18	2.226	4.000	HSS 5.0 × 0.375	18.5	5.1	4.3	1.04	36

simple to use given the current production tolerances. Based on the experimental and analytical investigation results, the following conclusions can be made;

1. The proposed splice sleeve is capable of developing of 100% of the ultimate strength of the spliced bars using a sleeve length of 16 times the bar diameter and using commercial available non-shrink high strength grout.
2. Internal threading of the sleeve with 1/8″ deep threads is adequate in preventing the slippage of the grout from the sleeve. Different thread depths could result in different performance and need to be tested.
3. Coefficient of friction can be conservatively assumed to be 1.0 in designing the proposed splice sleeve. Average measured coefficients of friction is approximately 1.6.
4. The shear friction method proposed for designing the bar splice sleeve is adequate.

7. Recommendations

Based on the design methodology presented in Section 3 and validated experimentally in Section 4, the authors recommend the splice sleeves shown in Table 4 for different bar sizes. This table indicates that the proposed splice sleeve provides an average tolerance of 1 in., which is favorable tolerance for precast production. It should be noted that additional testing is recommended to confirm the performance of splice sleeves for bar sizes other than #8 and #9, which were tested in this study.

It is also important to experimentally evaluate the performance of the proposed splice sleeve under cyclic loading (i.e. fatigue behavior) and in a full-scale setting (e.g. connecting wall panels) when necessary before implementation to ensure adequate performance based on application requirements.

References

[1] Adajar J, Yamaguchi T, Imai H. An experimental study on the tensile capacity of vertical bar joints in a precast shear wall. In: Proceedings of the 4th international conference on structural failure, durability and retrofitting, Singapore; 1993. p. 431–8.

[2] American Concrete Institute (ACI). Building code requirements for structural concrete and commentary. Farmington Hills, MI; 2011.

[3] Darwin D, Zuo J, Tholen ML, Idun EK. Development length criteria for conventional and high relative rib area reinforcing bars. ACI Struct J 1996;93(3):1–13.

[4] Einea A, Yamane T, Tadros MK. Grout-filled pipe splices for precast concrete construction. PCI J 1995;40(1):82–93.

[5] Einea A, Yehia S, Tadros MK. Lap splice in confined concrete. ACI Struct J 1999;96(6):947–55.

[6] Harries KA, Zeno G, Shahrooz B. Toward an improved understanding of shear-friction behavior. ACI Struct J 2012(6):835–44. V109.

[7] Orangun CO, Jirsa JO, Breen JE. A re-evaluation of test data on development length and splices. ACI J 1977;74(3):114–22.

[8] Sheikh SA, Toklucu MT. Reinforced concrete columns confined by circular spirals and hoops. ACI Struct J 1993;90(5):542–53.

[9] Soroushian P, Choi KB, Park GH, Aslani F. Bond of deformed bars to concrete: effects of confinement and strength of concrete. ACI Mater J 1991;88(3):227–32.

[10] Untrauer RE, Henry RL. Influence of normal pressure on bond strength. ACI J 1965;62(5):577–85.

[11] Zuo J, Darwin D. Splice strength of conventional and high relative rib area bars in normal and high-strength concrete. ACI Struct J 2000;97(4):630–41.